Journal of the European Ceramic Society 20 (2000) 1035–1041

The effects of La on the dielectric properties of lead iron tungstate $Pb(Fe_{2/3}W_{1/3})O_3$ relaxor ceramics

Liqin Zhou[a], P.M. Vilarinho[a], P.Q. Mantas[a], J.L. Baptista[a,*], E. Fortunato[b]

[a]*Department of Ceramics and Glass Engineering / UIMC, University of Aveiro, 3810 Aveiro, Portugal*
[b]*CENIMAT, Materials Science Department, Faculty of Science and Technology of New University of Lisbon, 2825 Monte de Caparica, Portugal*

Received 23 March 1999; received in revised form 10 September 1999; accepted 6 October 1999

Abstract

La doped samples were used to study the effects of this dopant on the structural and dielectric properties of $Pb(Fe_{2/3}W_{1/3})O_3$ (PFW) relaxor ceramics. La doping leads to a decrease in the lattice constant of the cubic PFW perovskite and to the precipitation of increasing amounts of a second phase, $PbWO_4$. A decrease of dielectric permittivity maximum, ε_{rmax}, a shift of transition temperature, T_0, to lower temperatures, and an increase of diffuseness, δ, are also observed. Undoped and La doped PFW show a p-type conduction. The resistivity vs La content shows a "V-like" curve. The aging behavior of the samples are also altered by the presence of the dopant. The aging decreases with increasing the La content up to 5 at% and increases after that. Charge compensation and defect associations in the La doped samples are discussed and suggested to explain the electrical properties and the aging behavior.

Keywords: Dielectric properties; Electrical resistivity; Lead iron tungstate; Perovskites; $Pb(Fe,W)O_3$

1. Introduction

Lead based perovskite $Pb(B'_{1-x}B''_x)O_3$ relaxors became, in the early 80s, very attractive and successful industrial materials for high capacitance multilayer capacitors, mainly because of their low sintering temperature (low cost electrodes can be used), high diffuse dielectric permittivity peak and the possibility of designing properties by making appropriate solid solutions between them.[1]

The understanding of the physical nature, responsible for the peculiar dielectric macroscopic characteristics of relaxors, typified by a high dielectric permittivity value, a diffuse phase transition, a strong relaxation of the dielectric properties with frequency, an absence of macroscopic polarization at temperatures far below the permittivity maximum temperature (transition temperature) and a characteristic aging behavior, became a scientific subject of interest, not completely established until now.

Many authors at different times proposed several models to explain the ferroelectric relaxor behavior. Among them, the compositional fluctuation model,[2] the superparaelectric model,[3] the dipolar glass model[4] and the random field model[5] have received the most attention. Recently, it was observed that the size of the domains and the degree of B cation order of $Pb(Mg_{1/3}Ta_{2/3})O_3$ (PMT) can be significantly increased by annealing at high temperatures and that fully ordered ceramics that were comprised of large domains still retained the relaxor behavior.[6] This experimental evidence points out that there is no direct correspondence between the micro/nano scale of polar regions and the relaxor behavior.

In spite of its low transition temperature, around 185 K,[7] $Pb(Fe_{2/3}W_{1/3})O_3$ (PFW) is used to obtained solid solutions with other relaxor compositions, allowing these compositions to meet standard specifications for multilayer capacitors. It is conceivable that it can also be a material of choice for components subject to low temperatures for extended periods of time. PFW exhibits typical relaxor properties.[7] No long range order was identified in PFW,[8] pointing out for a disordered structure in which the Fe^{3+} and W^{6+} ions are randomly distributed on the octahedral positions.

For practical applications, it is imperative to guarantee minimal dielectric losses and minimal dielectric

* Corresponding author.

0955-2219/00/$ - see front matter
PII: S0955-2219(99)00277-0

aging. Some studies on PFW ceramics[9,10] showed clear changes of the dielectric properties and aging behavior for defective PFW compositions, stressing the influence, on the relaxor behavior, of the lattice defects and their spatial positions and supporting the idea, discussed for other lead based materials, like lead lanthanum zirconate titanate (PLZT)[11,12] and $Pb(Mg_{1/3}Nb_{2/3})O_3$ (PMN)[13], that a lattice defect constitutes the essential ingredient for the aging process.

In order to clarify some characteristics of the dielectric behavior of this relaxor, lanthanum doped PFW samples were prepared and investigated, in the present work. The role of the La incorporation in PFW is discussed both from the structural point of view and from the electrical one, namely its effect on dc resistivity, diffuse phase transition and dielectric aging.

2. Experimental

The La incorporated into PFW ceramics were considered to substitute Pb on the A sites. The compositions studied are represented by the general formulas $Pb_{1-x}La_x(Fe_{2/3}W_{1/3})O_3$ in which $x = 0$, 0.005, 0.01, 0.03, 0.05, 0.07, 0.1 and 0.12 and $Pb_{1-y}La_y[(Fe_{(2+y)/3}W_{(1-y)/3})O_3$ in which $y = 0.05$ and 0.1.

All the samples, indicated in Table 1, were prepared by the columbite precursor method, as previously described.[14] Reagent grade Fe_2O_3 and WO_3 were first ball-milled in alcohol for 4 h, dried, prereacted at 1000°C for 2 h, and then ball-milled with PbO and La_2O_3. After the calcination at 800°C for 2 h, the powders were ball-milled again in alcohol for 10–15 h, to obtain powders of less than 5 μm of particle size. Pellets of 10mm in diameter and 2–3 mm in thickness were uniaxially pressed at 100 MPa and then isostatically pressed at 300 MPa. The samples were sintered at 870°C for 2 h.

The density of the sintered samples was determined according to Archimedes principle, using an analytical balance and diethyl phthalate as the reference liquid.

Some of the sintered samples were ground into powder and the phases were identified by X-ray diffraction analysis. The microstructures of the samples were observed in polished sections, as well as the composition analysis by energy dispersion spectroscopy (EDS), using scaning electron microscopy (S.E.M.).

Hall effect measurements were carried out to check the nature of the main carrier in PFW and in the La doped PFW. The measurements were done at room temperature with four Ag electrodes, following the Van der Pauw geometry. The magnetic field was 0.5 T and for each measurement, the values were taken before and after reversing the magnetic field direction and the current direction, under low electric field (less than 0.03 V/cm) condition. For each measurement, an average of 10 cycles was taken.

For the dielectric measurements, sintered samples were polished and gold electrodes were sputtered on both sides. Dielectric permittivity and loss factor were measured, at 10 kHz, as a function of temperature, during heating-up at a rate of 1 K min^{-1}, using a Solartron 1260 impedance/gain-phase analyzer and a Displex APD-cryogenics cryostat. Dc resistivity was measured at room temperature with a Keithley 617 Programmable Electrometer.

The diffuseness coefficient, δ, which characterizes the breadth of the diffuse ferroelectric / paraelectric transition, was calculated by the Gaussian distribution relation:[15]

$$\varepsilon_{rmax}/\varepsilon_r = \exp\left[(T - T_0)^2/2\delta^2\right],$$

where ε_{rmax} is the dielectric permittivity maximum, ε_r the dielectric permittivity at T and T_0 the temperature at which ε_{rmax} occurs (transition temperature).

Before the aging treatment, a capacitance-temperature run was done. The samples were heated to room temperature to relieve any earlier aging effect and then cooled to the aging temperature (143 K). Isothermal aging of the samples was conducted in the cryostat chamber at 143 K for 100 h, under open circuit conditions. After that, the samples were rapidly cooled to 50 K and the dielectric properties were measured during heating up at a rate of 1 K min^{-1}.

Table 1
Sintering characteristics of $Pb_{1-x}La_x(Fe_{2/3}W_{1/3})O_3$ and $Pb_{1-y}La_y[(Fe_{(2+y)/3}W_{(1-y)/3})]O_3$ ceramics

Designation	Compositions	Weight loss (%)	Grain size (μm)
PFW	$Pb(Fe_{2/3}W_{1/3})O_3$	0.32	2.1
PFW–0.5La	$Pb_{1-x}La_x(Fe_{2/3}W_{1/3})O_3$, $x = 0.5$ at%	0.30	2.1
PFW–1La	$Pb_{1-x}La_x(Fe_{2/3}W_{1/3})O_3$, $x = 1$ at%	0.27	2.3
PFW–3La	$Pb_{1-x}La_x(Fe_{2/3}W_{1/3})O_3$, $x = 3$ at%	0.24	2.4
PFW–5La	$Pb_{1-x}La_x(Fe_{2/3}W_{1/3})O_3$, $x = 5$ at%	0.22	2.4
PFW–7La	$Pb_{1-x}La_x(Fe_{2/3}W_{1/3})O_3$, $x = 7$ at%	0.20	2.6
PFW–10La	$Pb_{1-x}La_x(Fe_{2/3}W_{1/3})O_3$, $x = 10$ at%	0.18	2.8
PFW–12La	$Pb_{1-x}La_x(Fe_{2/3}W_{1/3})O_3$, $x = 12$ at%	0.17	2.9
PFW–5La(2)	$Pb_{1-y}La_y[(Fe_{(2+y)/3}W_{(1-y)/3})]O_3$, $y = 5$ at%	0.20	2.5
PFW–10La(2)	$Pb_{1-y}La_y[(Fe_{(2+y)/3}W_{(1-y)/3})]O_3$, $y = 10$ at%	0.19	3.0

3. Results

The XRD patterns of PFW, PFW–1La, PFW–5La and PFW–12La are presented in Fig. 1. Besides the PFW perovskite phase, trace amounts of second phases, $PbWO_4$ and $Pb_2FeWO_{6.5}$, are observed in PFW ceramics, as previously reported,[14] while only the $PbWO_4$ second phase is detected in the La doped $Pb_{1-x}La_x(Fe_{2/3}W_{1/3})O_3$ samples and its amount increases with the increase in the La content. The second phases could not be observed in the S.E.M. pictures.

The cubic lattice constant (a_0) of the $Pb_{1-x}La_x(Fe_{2/3}W_{1/3})O_3$ compositions, shown in Fig. 2, were determined from their diffraction patterns. A clear linear decrease of a_0 is observed. This supports the assumption that the La ions were incorporated into the PFW perovskite lattice, substituting for Pb^{2+}. The decrease of a_0 with La content could be due to the smaller ionic radius of La^{3+} (1.32 Å[16,17]) compared to that of Pb^{2+} (1.49 Å[16,17]).

The sintering characteristics of $Pb_{1-x}La_x(Fe_{2/3}W_{1/3})O_3$ ceramics are represented in Table 1. Small weight losses were observed for all the samples, decreasing systematically when Pb^{2+} is substituted by La^{3+}. High degrees of densification, between 92 and 97% of theoretical density, could be inferred by S.E.M. observation of polished surfaces.

The microstructures of the PFW and PFW-5La samples are shown in Fig. 3. There is a tendency for a small increase in the grain size for La doped samples (Table 1).

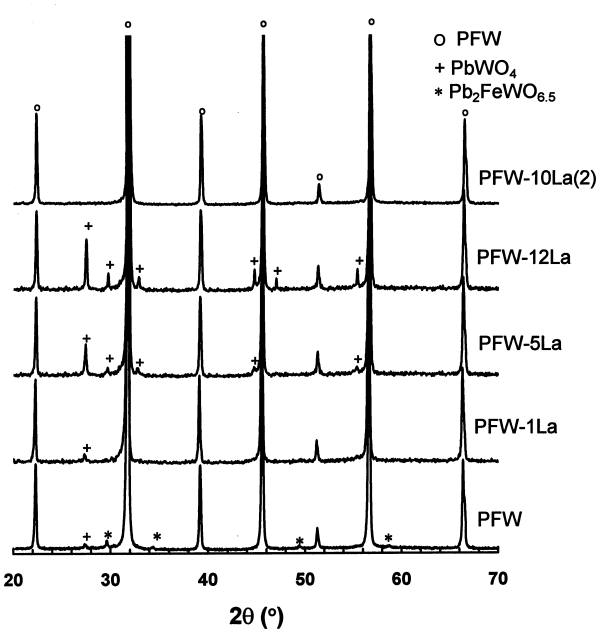

Fig. 1. XRD patterns of La modified PFW ceramics.

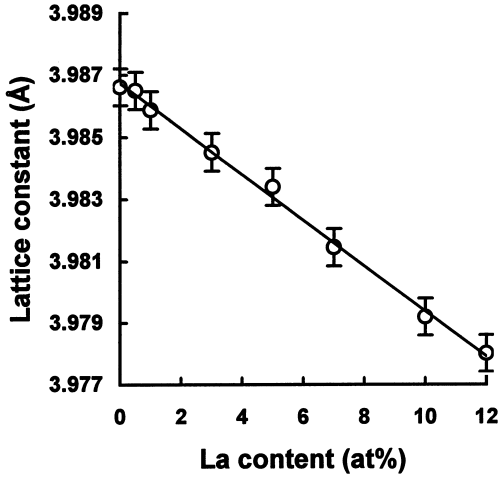

Fig. 2. Dependence of the lattice constant of $Pb_{1-x}La_x(Fe_{2/3}W_{1/3})O_3$ on La content.

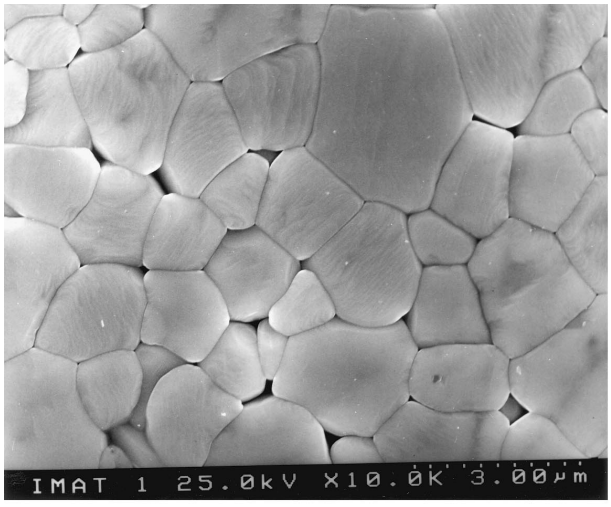

(a)

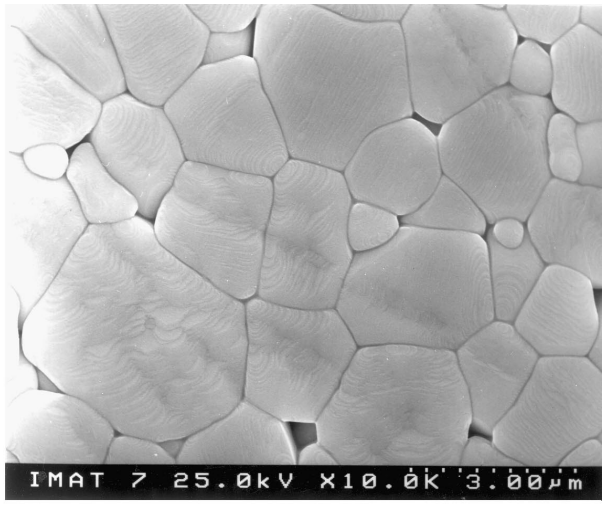

(b)

Fig. 3. S.E.M. microstructures of PFW (a) and PFW–5La (b) ceramics.

Although a reliably quantitative elements analysis is difficult to obtain by EDS/S.E.M., an increase in the amount of lanthanum in the matrix grains with the increase of La content in the samples was observed, confirming that the La ions are incorporated into the PFW lattice. Moreover, a decrease in the matrix grains of the tungsten amount as the La amount increased was also found, in agreement with the observed precipitation of $PbWO_4$.

The dielectric properties of the $Pb_{1-x}La_x(Fe_{2/3}W_{1/3})O_3$ compositions are shown in Table 2, stressing the effects of the La doping on the dielectric behavior of PFW ceramics. The increase in the La content results in a pronounced decrease of the dielectric permittivity maximum, ε_{rmax}, a shift of the transition temperature, T_0, to lower temperatures, and an increase of the diffuseness coefficient, δ.

Hall effect measurements show that the main charge carrier of undoped and La doped PFW is the electron hole. This can be attributed to the ionization of lead vacancies originated from lead loss during sintering,

$$V_{Pb} \Longleftrightarrow V_{Pb}'' + 2h^{\bullet} \quad (1)$$

where V_{Pb}'' is a doubly ionized lead vacancy and $h^{\bullet}$ a hole.

The dc resistivity of $Pb_{1-x}La_x(Fe_{2/3}W_{1/3})O_3$ ceramics decreases for increasing amounts of La, until 5 at% of La, increasing after that until 10 at% and then remaining almost unchanged for higher La amounts. This behavior becomes clearer from the plot of resistivity vs La content (Fig. 4), where a "V-like" curve is displayed.

The dielectric permittivity and loss factor, as a function of temperature, at 10 kHz, for the PFW, PFW-0.5La, PFW–1La, PFW–5La and PFW–10La compositions are shown in Fig. 5. The variations of the dielectric parameters as a function of the La content, pointed in Table 2, become evident.

In the loss factor curves (Fig. 5b), a well defined second peak, with high loss values, can be observed for all the samples. The same effect was observed in the $\varepsilon_r = f(T)$ curves, but for higher temperatures not plotted in Fig. 5a. Although the nature of these second peaks is not under discussion in this work, it is worthwhile to emphasize that the highest loss peak corresponds to the PFW–5La sample and the lowest to the PFW–10La one, exactly the samples that show the lowest and the highest dc resistivity values, respectively (Fig. 4).

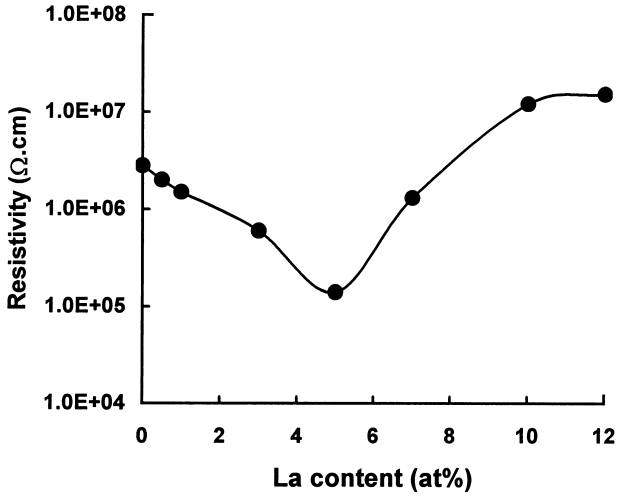

Fig. 4. Dependence of resistivity of $Pb_{1-x}La_x(Fe_{2/3}W_{1/3})O_3$ ceramics on La content.

The graphical variations of the dielectric permittivity (ε_r) and loss factor (tanδ) against temperature, for aged and unaged samples of PFW–0.5La are presented in Fig. 6. As can be seen, the aged curves are distorted near the aging temperature (143 K), specially in the loss factor curves, showing an aging distortion similar to that of nonstoichiometric[9] and Mn-doped[10] PFW, PLZT[11,12] and PMN[13] ceramics. The aging level decreases with the increase in the La content up to 5 at%. No aging distortion was observed for the 5 at% La sample, this occurring again for the PFW–10La composition. This tendency

Table 2
Dielectric properties of $Pb_{1-x}La_x(Fe_{2/3}W_{1/3})O_3$ and $Pb_{1-y}La_y[(Fe_{(2+y)/3}W_{(1-y)/3})]O_3$ ceramics

Designation	ε_{rmax}	T_0 (K)	δ (K)	Resitivity (Ω·cm)	Percentage of aging[a] (at 143 K) (%)	
					$\Delta\varepsilon_r/\varepsilon_r$	Δtanδ/tanδ
PFW	12180	185	53	2.8×10^6	4.4	11.3
PFW–0.5La	9630	182	57	2.0×10^6	3.2	10.9
PFW–1La	8810	176	62	1.5×10^6	2.4	9.4
PFW–3La	5900	162	78	6.0×10^5	1.5	5.1
PFW–5La	4560	153	91	1.4×10^5	No aging	No aging
PFW–7La	2980	150	110	1.3×10^6	2.9	7.8
PFW–10La	1500	148	190	1.2×10^7	3.6	10.8
PFW–12La	1200	145	194	1.5×10^7	—[b]	—
PFW–5La(2)	5110	140	84	3.0×10^7	—	—
PFW–10La(2)	3000	120	173	2.5×10^7	—	—

[a] Aging at 143 K for 100 h.
[b] —, Not measured.

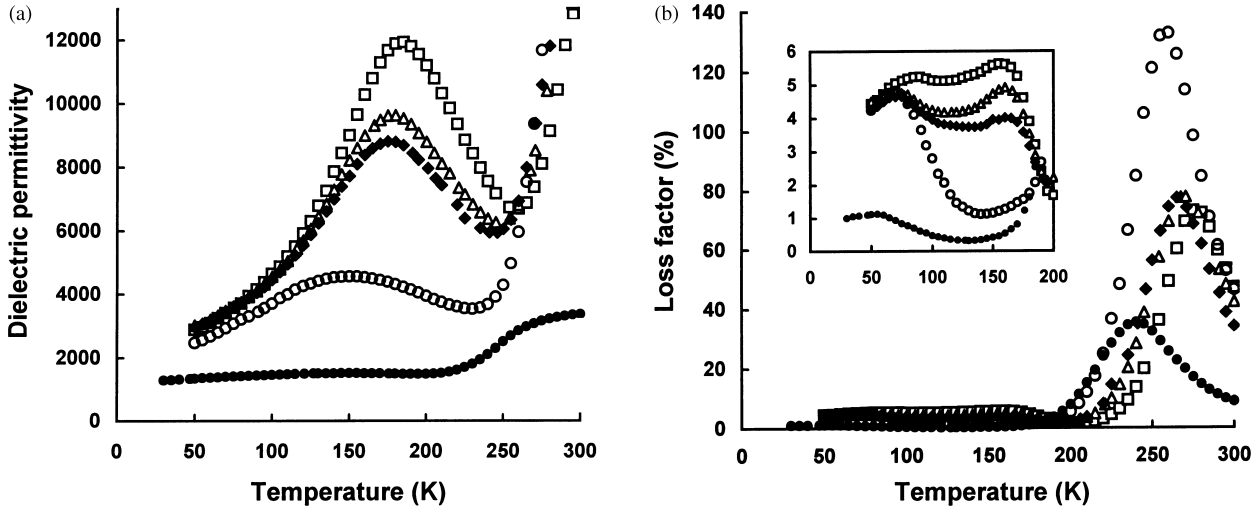

Fig. 5. Dielectric permittivity (a) and loss factor (b) as a function of temperature, at 10 kHz, for PFW (□), PFW–0.5La (△), PFW–1La (◆), PFW–5La (○) and PFW–10La (●). Insert is the expansion of the loss factor curves in the 0–200 K temperature region.

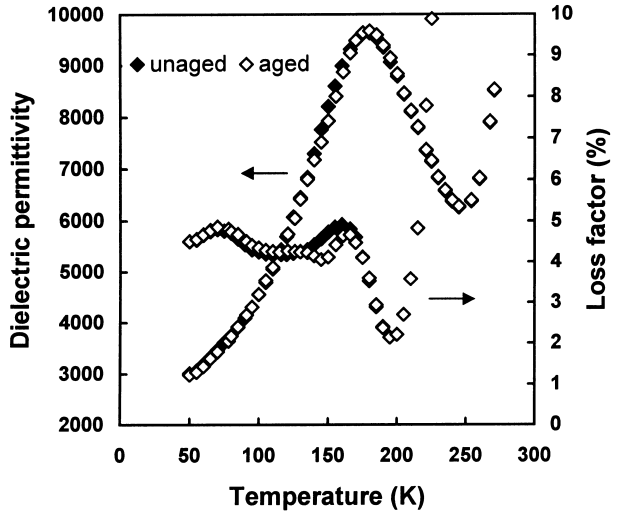

Fig. 6. Dielectric permittivity and loss factor as a function of temperature, at 10 kHz, for unaged and aged PFW–0.5La (aging at 143 K for 100 h).

can be seen from Table 2, where the percentage of aging ($\Delta\varepsilon_r/\varepsilon_r$ and $\Delta\tan\delta/\tan\delta$, where $\Delta\varepsilon_r = \varepsilon_r - \varepsilon_{ra}$, ε_r and ε_{ra} being the permittivity values at the aging temperature for the same sample before and after aging, with similar relations for the loss factor) are tabulated.

4. Discussion

According to the results presented above, in the $Pb_{1-x}La_x(Fe_{2/3}W_{1/3})O_3$ ($x \leqslant 12\%$) system, the La ions were incorporated into the PFW perovskite lattice. The linear decrease of the lattice constant supports the assumption of substitution in the A site position.

By analogy to other ABO_3 perovskites, like $BaTiO_3$,[18] the La ions located at Pb sites carry excess positive charges which, in order to maintain charge balance, usually are considered to be compensated by electrons and/or A-site vacancies,

$$La_{Pb} \Longleftrightarrow La_{Pb}^{\bullet} + e' \quad (2)$$

$$La_{Pb} \Longleftrightarrow La_{Pb}^{\bullet} + 1/2V_{Pb}'' \quad (3)$$

where $La_{Pb}^{\bullet}$ is an ionized La donor, V_{Pb}'' a doubly ionized lead vacancy and e′ an electron.

If the electron compensation [Eq. (2)] takes place, it will decrease the hole concentration and thus increase the resistivity. The lead vacancy compensation [Eq. (3)], having no contribution to the carrier concentration, should have almost no influence on the resistivity.

$Pb_{1-x}La_x(Fe_{2/3}W_{1/3})O_3$ decreases as the amount of La doping increases, as can be seen in Table 1. This will lead to an increase in the resistivity. So, either the electron compensation for La^{3+} substituting Pb^{2+} or the decrease in lead loss with La dopant will cause a monotonous increase in the resistivity with increasing the La content, which was not experimentally observed. The resistivity of the $Pb_{1-x}La_x(Fe_{2/3}W_{1/3})O_3$ changes with the La content in a "V-like" way, as shown in Fig. 4. The resistivity decreases for low La contents, reaching a minimum for La = 5 at% and increases thereafter until La = 10 at%.

To interpret the resistivity variations, the compositional changes occurring in the $Pb_{1-x}La_x(Fe_{2/3}W_{1/3})O_3$ samples have also to be considered. As described above, the tungsten amount in the matrix grains decreases as the La content increases with concomitant precipitation of $PbWO_4$. The difficiency in tungsten results in a net negative charge excess on the B sites. Theoretically, this excess charge could be completely compensated if the composition would be readjusted according to the formula $Pb_{1-y}La_y[(Fe_{(2+y)/3}W_{(1-y)/3})]O_3$. So, in the $Pb_{1-x}La_x(Fe_{2/3}W_{1/3})O_3$ ceramics, where a stoichiometric

proportion of Fe/W (2:1) was introduced in the sample preparation and a higher Fe/W ratio would be present after sintering, the relative excess of tungsten should form a second phase, as it was indeed observed. The $PbWO_4$ second phase was detected for all the $Pb_{1-x}La_x(Fe_{2/3}W_{1/3})O_3$ samples, as shown in Fig. 1.

Following this idea, the ceramics with the compositional formula $Pb_{1-y}La_y[(Fe_{(2+y)/3}W_{(1-y)/3})]O_3$ must be monophasic. To confirm this idea, samples having a composition given by the formula $Pb_{1-y}La_y[(Fe_{(2+y)/3}W_{(1-y)/3})]O_3$, in which $y = 0.05$ and 0.1 [designated as PFW–5La(2) and PFW–10La(2), respectively], were prepared. A pure perovskite PFW phase was observed in both of these compositions, as shown in Fig. 1, for PFW–10La(2). The dielectric properties of PFW–5La(2) and PFW–10La(2) ceramics are also shown in Tables 1 and 2. The formation of the second phase $PbWO_4$ in $Pb_{1-x}La_x(Fe_{2/3}W_{1/3})O_3$ can also be taken as supporting the charge compensation mechanism described by Eq. (3) which, with simultaneous production of extra tungsten vacancies will create holes by their ionization, thus decreasing the resistivity. The higher resistivity values of PFW–5La(2) and PFW–10La(2) samples where no $PbWO_4$ second phase was observed seem to support this suggestion.

The "V-like" variation in resistivity shown in Fig. 4 is then probably a result of the competition of the decrease of the resistivity caused by the $PbWO_4$ phase formation and the increase of the resistivity due to the decrease of the lead loss and/or the electron compensation occurrence by Eq. (2).

The lattice change due to the readjustment of Fe/W can be negligible since the ionic radius of Fe^{3+} (0.55 Å[16,17]) and W^{6+} (0.58 Å[16,17]) are similar. It was observed that the lattice constant of the perovskite of PFW–5La(2) and PFW–10La(2) is similar to that of PFW–5La and PFW–10La respectively.

Turning now to the aging behavior of $Pb_{1-x}La_x(Fe_{2/3}W_{1/3})O_3$ ceramics (Fig. 6 and Table 2), it is interesting to note that the change of the aging level with the La content shows a similar behavior as that of resistivity (Fig. 4 and Table 2). When La < 5 at%, both the resistivity and the aging level decrease with the increase in the La content. The resistivity reaches a minimum at La = 5 at%, while no aging is observed. For the composition with La = 10 at%, the resistivity increases and the aging appears again.

Aging has been correlated with the presence of polar defect pairs.[9–13] It was attributed to the coupling of the defect pairs to the polarization vectors in the nanodomains, stabilizing the existing domain states.[9–13] The easiness of the reorientation of defect pairs was suggested to be responsible for the various aging degrees of nonstoichiometric[9] and Mn doped[10] PFW ceramics.

In stoichiometric PFW ceramics if the holes originated from Eq. (1) weakly bind to Fe^{3+} originating $Fe^{3+}\cdot h$ ($Fe^{\bullet}_{Fe}$), their associations with lead vacancies to form polar defect pairs $V_{Pb}''-Fe^{\bullet}_{Fe}$ will originate the defect pair that can be used to explain the aging in stochiometric PFW. The easy reorientation of these pairs will correspond to an electron (hole) jump between two Fe ions, a process similar to the small polaron contribution to conductivity. Fe^{4+} has been detected by optical means in perovskite lattices containg Fe.[19] Also Fe^{4+} was found using Mossbauer in heavily Fe doped $SrTiO_3$.[20] Although the detection of different Fe oxidation states in our samples was tried using Mossbauer spectroscopy, this was not successful due to the lower Fe content of PFW and the shielding effect of Pb and W.

As the La concentration is increasing (La ⩽ 5 at%), it is conceivable that the association $V_{Pb}''-La^{\bullet}_{Pb}$ will progressively become dominant. Its difficulty in reorientating, which will correspond to Pb diffusion in the perovskite lattice will not allow its coupling to the polarization vectors of the nanodomains of the relaxor, maintaining therefore the capability of these polarization vectors to follow the applied field.

At higher La concentration (La > 5 at%) it seems that another more mobile defect pair is being created, since the aging of these high doped samples is again detected. It is probably correlated again with the oxidation-reduction equilibrium process of the Fe ions.

In $Pb_{1-x}La_x(Fe_{2/3}W_{1/3})O_3$ ceramics, when the La content increases, the composition of the matrix grains goes towards $Pb_{1-y}La_y[Fe_{(2+y)/3}W_{(1-y)/3}]O_3$, as suggested, and the amount of the second phase, $PbWO_4$, increases (Fig. 1). The smaller permittivity and higher diffuseness coefficient of the $Pb_{1-y}La_y[Fe_{(2+y)/3}W_{(1-y)/3}]O_3$ compositions (Table 2) lead to the decrease of ε_{max} and the increase of δ, with increase in La content, of the $Pb_{1-x}La_x(Fe_{2/3}W_{1/3})O_3$ ceramics, as shown in Table 2. Moreover, the second phase $PbWO_4$ in $Pb_{1-x}La_x(Fe_{2/3}\ W_{1/3})O_3$ ceramics may also effectively decrease the permittivity of the ceramics.

X-ray analysis (Fig. 2) shows that an increase of La^{3+} concentration causes a decrease of the lattice parameter, thus of the unit cell volume, thereby leading to a shift of T_0 to lower temperatures in the same manner as an hydrostatic pressure.[21]

5. Conclusions

Doping PFW ceramics with La modifies markedly its dielectric properties. La doping results in a decrease of ε_{rmax}, a shift of T_0 to lower temperatures and an increase of δ. With increasing the La content, the resistivity decreases below 5 at%, increases above 5 at%, and then remains constant above 10 at%, showing a "V-like" curve. The observed variation in resistivity is suggested to be a result of the competition of the decrease of the resistivity caused by the $PbWO_4$ phase formation and the

increase of the resistivity due to the decrease of the lead loss and/or the electron compensation occurrence.

The aging decreases with increasing La content up to 5 at% and increases again after that. The role played by the possible defect associations present in La doped samples, on their aging behaviors, is discussed.

Acknowledgements

The authors acknowledge the FCT (Portuguese Foundation for Science and Technology) for financial support and one of them (L.Z.) thanks Praxis XXI for a maintenance grant.

References

1. Shrout, T. R. and Halliyal, A., Preparation of lead-based ferroelectric relaxors for capacitors. *Am. Ceram. Soc. Bull.*, 1987, **66**(4), 704–711.
2. Smolenskii, G. A., Isupov, V. A., Agranovskaya, A. I. and Popov, S. N., Ferroelectrics with diffuse phase transition. *Sov. Phys. Solid State*, 1961, **2**, 2584–2594.
3. Cross, L. E., Relaxor ferroelectrics. *Ferroelectrics*, 1987, **76**, 241–267.
4. Viehland, D., Li, J. F., Jang, S. J. and Cross, L. E., Dipolar-glass model for lead magnesium niobate. *Phys. Rev. B*, 1991, **43**(10), 8316–8320.
5. Westphal, V., Kleemann, W. and Glinchuk, M. D., Diffuse phase transitions and random-field-induced domain states of the relaxor ferroelectric $PbMg_{1/3}Nb_{2/3}O_3$. *Phys. Rev. Lett.*, 1992, **68**, 847–850.
6. Akbas, M. A. and Davies, P. K., Domain growth in $Pb(Mg_{1/3}Ta_{2/3})O_3$ perovskite relaxor ferroelectric oxides. *J. Am. Ceram. Soc.*, 1997, **80**, 2933–2936.
7. Vilarinho, P. M. and Baptista, J. L., Effect of excess of iron oxide and lead oxide on the microstructure and dielectric properties of lead iron tungstate ceramics. *J. Eur. Ceram. Soc.*, 1993, **11**, 407–411.
8. Liqin, Zhou., Vilarinho, P. M. and Baptista, J. L., Effects of annealing treatment on the dielectric properties of Mn modified $Pb(Fe_{2/3}W_{1/3})O_3$ ceramics. *J. Mat. Sci.*, 1998, **33**, 2673–2677.
9. Liqin, Zhou., Vilarinho, P. M. and Baptista, J. L., Stoichiometric dependence of the aging phenomena in lead iron tungstate ceramics. *J. Am. Ceram. Soc.*, 1996, **79**(9), 2436–2442.
10. Liqin, Zhou., Vilarinho, P. M. and Baptista, J. L., Dielectric properties and aging effects of manganese modified lead iron tungstate relaxor ceramics. *Mater. Res. Bull.*, 1996, **31**(6), 699–708.
11. Schulze, W. A. and Biggers, J. V., Dielectric aging in the PLZT system. *Ferroelectrics*, 1975, **9**(3-4), 203–207.
12. Schulze, W. A., Biggers, J. V. and Cross, L. E., Aging of dielectric dispersion in PLZT relaxor ceramics. *J. Am. Ceram. Soc.*, 1978, **61**(1-2), 46–49.
13. Pan, W., Furman, E., Dayton, G. O. and Cross, L. E., Dielectric aging effects in doped lead magnesium niobate: lead titanate relaxor ferroelectric ceramics. *J. Mat. Sci. Lett.*, 1989, **5**, 647–649.
14. Liqin, Zhou., Vilarinho, P. M. and Baptista, J. L., Synthesis and characterization of lead iron tungstate ceramics obtained by two preparation methods. *Mater. Res. Bull.*, 1994, **29**(11), 1193–1201.
15. Pilgrim, S. M., Sutherland, A. E. and Winzer, S. R., Diffuseness as a useful parameter for relaxor ceramics. *J. Am. Ceram. Soc.*, 1990, **73**(10), 3122–3125.
16. Shannon, R. D. and Prewitt, C. T., Effective ionic radii in oxides and fuorides. *Acta Cryst.*, 1969, **B25**, 925–946.
17. Shannon, R. D. and Prewitt, C.T, Revised values of effective ionic radii. *Acta Cryst.*, 1970, **B26**, 1046–1048.
18. Saburi, O., Properties of semiconductive barium titanates. *J. Phys. Soc. Jap.*, 1959, **14**(9), 1159–1174.
19. Bieger, T., Maier, J. and Waser, R., Kinetics of oxygen incorporation in $SrTiO_3$ (Fe doped): an optical investigation. *Sensors and Actuators B*, 1992, **7**, 763–768.
20. Chen Ang et al., unpublised results.
21. Merz, W. J., The effect of hydrostatic pressure on the curie point of barium titanate single cystals. *Phys. Rev.*, 1950, **77**(7), 52–54.